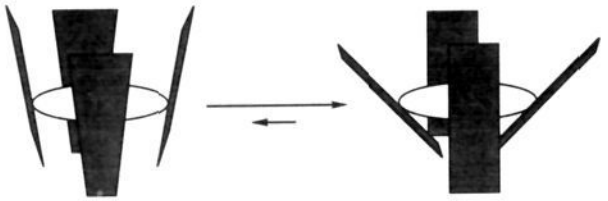

Figure 1. Stylized illustration of cone and pinched-cone conformational isomers of a calix[4]arene, showing the relative orientation of the aromatic moieties.

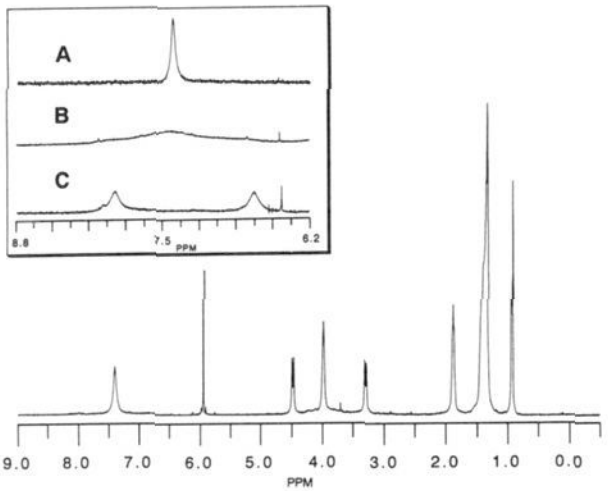

Figure 2. *^{1}H NMR (500 MHz) spectra of* **I** *in $CDCl_2CDCl_2$ at 100 °C;* insert shows aromatic protons at (A) 115 °C, (B) 45 °C, and (C) −4 °C. Residual solvent protons (δ 5.95) were used as an internal reference.

were isolated cone structures. Haloform oxidation of the former resulted in the formation of **I**; cyanation of the latter followed by hydrolysis yielded **II**.[11]

The ^{1}H NMR spectrum (500 MHz) of **I** that was observed in DMSO-d_6 at 23 °C gave a splitting pattern that was consistent with a cone (and also a rapidly equilibrating pinched cone) structure; i.e., a well-defined pair of doublets was observed for the bridging methylenes at δ 4.32 and 3.37 (J_{AB} = 13.0 Hz), and the aromatic protons appeared as a singlet at δ 7.30. In contrast, the ^{1}H NMR spectrum of **I** in $CDCl_2CDCl_2$ (23 °C) exhibited broadened resonances for the bridging methylenes (δ 3.3 and 4.4) and two broad signals for the aromatic protons of equal intensity (δ 6.7 and 8.0). The latter sharpened at lower temperatures, coalesced at 45 °C, and became a sharp singlet at higher temperatures (Figure 2). In addition, the oxymethylene protons, which appeared as a sharp absorption at higher temperatures (δ 4.0), were seen as two broad signals of equal intensity as the temperature was lowered (δ 4.1 and 3.7). The observed shielding of half of the aromatic and oxymethylene protons (and deshielding of the remaining half) at lower temperatures, together with this coalescence behavior, provides compelling evidence for pinched-cone conformers that are in dynamic equilibrium. On the basis of a coalescence temperature, T_c, of 45 °C and $\Delta\nu$ = 610 Hz, we calculate a barrier for interconvesion of $\Delta G^{\ddagger}$ = 14.1 kcal mol^{-1}.[12,13] Replacement of the carboxylic acid protons of **I** with deuterium afforded a T_c of 70 °C, $\Delta\nu$ = 660 Hz, and $\Delta G^{\ddagger}$ = 15.2 kcal mol^{-1}. Similar results were obtained with **II**; here, T_c = −4 °C, $\Delta\nu$ = 475 Hz, and $\Delta G^{\ddagger}$ = 13.3 kcal mol^{-1}; for deuterium-exchanged **II**, T_c = 15 °C, $\Delta\nu$ = 500 Hz, and $\Delta G^{\ddagger}$ = 14.2 kcal mol^{-1}. Finally, an analogous calix[4]arene, **III**, formed from **I** via CH_2N_2, "appeared" as a C_{4v} structure from −28 to 100 °C in $CDCl_2CDCl_2$.

The ability to observe C_{2v} symmetry for **I** and **II** by ^{1}H NMR spectroscopy clearly reflects the relatively high barrier for interconversion between the two pinched-cone conformers. On the basis of the *appearance* of **I** and **II** as cone structures in DMSO-d_6, the significant deuterium isotope effect on T_c, and the appearance of **III** as a C_{4v} structure in $CDCl_2CDCl_2$, we conclude that internal hydrogen bonding contributes, considerably, to this barrier. Previous molecular mechanics calculations have indicated that the C_{2v} conformer of 5,11,17,23-tetramethyl-25,26,27,28-tetramethoxycalix[4]arene is 3.2 kcal mol^{-1} lower in energy than the corresponding C_{4v} structure.[6] If a similar difference exists for the calix[4]arene framework in **I** and **II**, then the observed free energies of activation can be accounted for by assuming that *two* internal hydrogen bonds are formed between alternate pendant groups (contributing a total of ~10–11 kcal mol^{-1}) and that the C_{4v} structure represents a transition state for the interconversion.

As the level of sophistication in the design and synthesis of calix[4]arene-based hosts, templates, and pores increases, greater attention will have to be paid to the details of molecular structure and dynamics. Pinched-cone conformers will certainly require careful scrutiny in this regard.

Registry No. I, 137233-49-9; II, 137233-50-2; D_2, 7782-39-0.

(11) All new compounds showed the expected ^{1}H NMR (500 MHz) spectra and elemental analysis or HRMS.

(12) Lambert, J. B.; Shurvell, H. F.; Verbit, L.; Cooks, R. G.; Stout, G. H. *Organic Structural Analysis*; Macmillan Publishing: New York, 1976; p 117.

(13) Coalescence was also observed in THF-d_8 at −55 °C.

Structural Characterization of Mixed-Alkali-Metal Bis(trimethylsilyl)amide Bases

Paul G. Williard* and Michael A. Nichols

Department of Chemistry, Brown University
Providence, Rhode Island 02912

Received August 22, 1991

The enhanced deprotonating (or metalating) power of mixed organoalkali bases containing lithium and potassium or sodium over those containing only lithium was first observed by Wittig.[1] In the middle 1960s, Lochmann[2] and Schlosser[3] showed that very strong deprotonating reagents could be formed by combining equimolar mixtures of a potassium alkoxide with an alkyllithium compound. Despite an increasing number of syntheses which have utilized these "superbasic reagents",[4] relatively few physical organic studies[5] have been reported that have directly addressed the structure of the species responsible for their enhanced deprotonating ability. In recent years, however, solid-state structures of various mixed organoalkali compounds have been reported[6] in addition to the *n*-butyllithium–lithium *tert*-butoxide complex.[7]

In a related area, the addition of alkali-metal alkoxides to lithium amides also increases the deprotonating ability of the amide bases.[8,9] In our attempts to study mixed-alkali amide/alkoxide

(1) (a) Wittig, G.; Ludwig, R.; Polster, R. *Chem. Ber.* **1955**, *88*, 294. (b) Wittig, G.; Bickelhaupt, F. *Chem. Ber.* **1958**, *91*, 865. (c) Wittig, G.; Benz, E. *Chem. Ber.* **1958**, *91*, 873.

(2) Lochmann, L.; Pospisil, J.; Vodnansky, J.; Trekoval, J.; Lim, D. *Collect. Czech. Chem. Commun.* **1965**, *30*, 2187–2195.

(3) Schlosser, M. *J. Organomet. Chem.* **1967**, *8*, 9–16.

(4) For leading references to syntheses, see: Schlosser, M. *Pure Appl. Chem.* **1988**, *60*, 1627–1634.

(5) For leading references to physical organic studies, see: Lochmann, L.; Trekoval, J. *Collect. Czech. Chem. Commun.* **1988**, *53*, 76–96.

(6) (a) LiK(EtO$_2$CCHCO$_2$Et)[2.2.2-crypt]: Cambillau, C.; Bram, G.; Corst, J.; Riche, C. *Nouv. J. Chim.* **1979**, *3*, 9–11. (b) [Na(Me$_2$NCH$_2$CH$_2$NMe$_2$)]LiPh$_4$: Schumann, U.; Weiss, E. *Angew. Chem., Int. Ed. Engl.* **1988**, *27*, 584–585. (c) $(CH_3Na)_4\cdot(CH_3Li)_4$ (3/1): Weiss, E.; Sauermann, G.; Thirase, G. *Chem. Ber.* **1983**, *116*, 74–85. (d) Li_4Na_2[N=C(Ph)-*t*-Bu]$_6$: Barr, D.; Clegg, W.; Mulvey, R. E.; Smith, R. *J. Chem. Soc., Chem. Commun.* **1989**, 57–58. (e) $LiNa_3\{O{=}P(NMe_2)_3\}_3[N{=}C(NMe_2)_2]_4$: Clegg, W.; Mulvey, R. E.; Snaith, R.; Toogood, G. E.; Wade, K. *J. Chem. Soc., Chem. Commun.* **1986**, 1740–1741. (f) NaK(2-hydroxybenzoate)$_2$·(dibenzo-24-crown-8): Momany, C.; Hackert, M. L.; Sharma, J.; Poonia, N. S. *J. Inclusion Phenom.* **1987**, *5*, 3443–3445. (g) $Li_4K_4(Me_3COCH_2^-)_4(t\text{-}BuO^-)_4(THF)_3\cdot KOH$: Williard, P. G.; MacEwan, G. J. *J. Am. Chem. Soc.* **1989**, *111*, 7671–7672.

(7) Marsch, M.; Harms, K.; Lochmann, L.; Boche, G. *Angew. Chem., Int. Ed. Engl.* **1990**, *29*, 308–309.

0002-7863/91/1513-9671$02.50/0

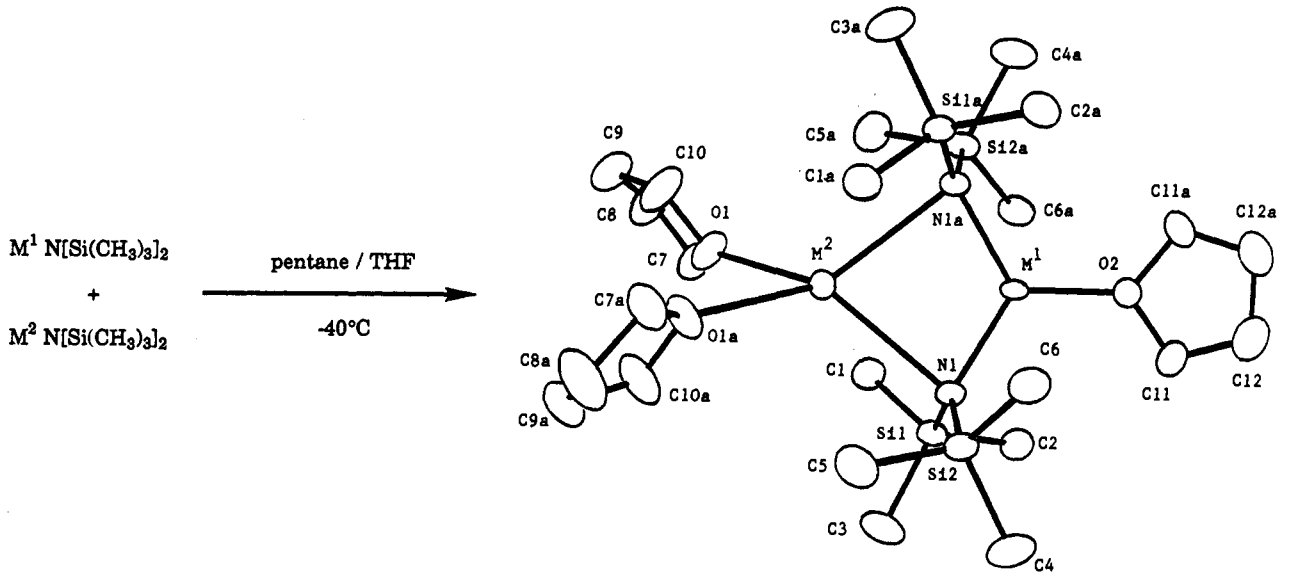

Bond Distance (in Å)

Compound	M^1	M^2	M^1-N	M^1-O	M^2-N	M^2-O
1	Li	K	2.053 (5)	1.926 (9)	2.832 (3)	2.689 (3)
2	Li	Na	2.024 (6)	1.964 (9)	2.509 (4)	2.433 (3)
3	Na	K	2.365 (3)	2.292 (3)	2.810 (3)	2.709 (3)

Figure 1. Generalized form of the structures of the mixed-alkali-metal HMDS bases 1–3. Further X-ray crystallographic data can be found in the supplementary material.

complexes in the solid state and in solution, we obtained three mixed lithium, sodium, and potassium bis(trimethylsilyl)amide (hexamethyldisilazanide, HMDS) bases and were able to determine their solid-state structures by X-ray diffraction analysis. The various mixed-alkali HMDS complexes were prepared by mixing equimolar amounts of the solid bases[10] in pentane (~0.1 M) and adding THF dropwise until a homogeneous solution was obtained. (See Figure 1.) Single crystals suitable for X-ray diffraction analysis were obtained upon cooling to −40 °C for 12–24 h.

The generalized structure[11] for the Li(HMDS)·K(HMDS)·3THF (**1**),[12] Li(HMDS)·Na(HMDS)·3THF (**2**),[13] and Na(HMDS)·K(HMDS)·3THF (**3**)[14] complexes is shown in Figure 1. All of the alkali HMDS bases are dimeric in the solid state, with the degree of THF solvation dependent upon the ionic radius of the alkali-metal cation such that the cation with the larger ionic radius is bissolvated and the smaller cation is monosolvated. The (M^1–N–M^2–N) cyclic rings of these complexes are planar (as required by the crystallographically imposed symmetry) and are slightly distorted when compared to the symmetric dimeric HMDS structures which contain only lithium[15] or potassium.[16] The distortions in the metallocyclic rings of compounds **1**, **2**, and **3** are due to different lithium–, sodium–, and potassium–nitrogen bond distances.

These mixed-alkali HMDS·3THF structures provide insight into some of the general structural features that may be present in complexes formed when potassium alkoxides are mixed with Li(HMDS) or other lithium amides in the presence of THF.[17,18] Results from our ongoing studies involving the solid-state and solution structures of mixed-alkali amide/alkoxide bases, as well as the relative reactivity of these bases compared with their pure lithium or potassium counterparts, will be reported in the future.

Acknowledgment. This work is supported by the National Institutes of Health through Grants GM-35982 and a Research Career Development Award (CA-01330) to P.G.W. The X-ray equipment was purchased with assistance from an instrument grant from the National Science Foundation (CHE-8206423).

(8) (a) Raucher, S.; Koolpe, G. A. *J. Org. Chem.* **1978**, *43*, 3794. (b) Renger, B.; Hugel, H.; Wykpiel, W.; Seebach, D. *Chem. Ber.* **1978**, *111*, 2630–2645.

(9) Lochmann, L.; Trekoval, J. *J. Organomet. Chem.* **1979**, *179*, 123–132.

(10) The solid HMDS bases were purified as described in the following: Nichols, M. A.; McPhail, A. T.; Arnett, E. M. *J. Am. Chem. Soc.* **1991**, *113*, 6222–6233.

(11) The three crystal structures are isomorphous with slight deviations in the conformations of the THF molecules.

(12) The mixed-alkali HMDS dimer $C_{24}H_{60}KLiN_2O_3Si_4$ (**1**) crystallizes in the monoclinic system, space group $C2/c$ (C^6_{2h}, No. 15) with a = 11.411 (3) Å, b = 20.546 (6) Å, c = 15.838 (5) Å, β = 96.68 (2)° (from 25 orientation reflections, 24° < 2θ < 26°), V = 3688 (2) Å^3, Z = 4, d_{calcd} = 1.05 g cm^{-3}, μ(Mo Kα) = 2.92 cm^{-1}. Intensity data ($\pm h,k,l$; 2427 nonequivalent reflections; θ_{max} = 45°) were recorded on a Nicolet R_3m/E diffractometer (Mo Kα radiation, λ = 0.710 69 Å; graphite monochromator, $\theta/2\theta$ scans) at approximately −80 °C under a stream of nitrogen gas. The crystal structure was solved by direct methods (SHELXS-86). Blocked-cascade least-squares refinement (SHELXTL 5.1) of atomic parameters (anisotropic C, N, Si, Li, O; fixed H contributions) converged (maximum shift 0.01σ) at R = 0.052 (R_w = 0.054, GOF = 1.93) over 1983 reflections with $I > 3.0\sigma(I)$. Further details for all structures are provided as supplementary material.

(13) Crystal data for $C_{24}H_{60}LiN_2NaO_3Si_4$ (**2**): monoclinic system; space group, $C2/c$; a = 11.368 (5) Å; b = 20.077 (13) Å; c = 16.203 (9) Å; β = 101.27 (4)°; V = 3629 (3) Å^3; Z = 4; d_{calcd} = 1.04 g cm^{-3}; μ(Mo Kα) = 1.94 cm^{-1}. Intensity data $\pm h,k,l$; 2372 nonequivalent reflections (θ_{max} = 45°); R = 0.057 (R_w = 0.056, GOF = 1.88) over 1790 reflections with $I > 3.0\sigma(I)$.

(14) Crystal data for $C_{24}H_{60}KN_2NaO_3Si_4$ (**3**): monoclinic system; space group $C2/c$; a = 11.588 (5) Å; b = 20.798 (9) Å; c = 15.756 (10) Å; β = 98.14 (4)°; V = 3759 (3) Å^3; Z = 4; d_{calcd} = 1.05 g cm^{-3}; μ(Mo Kα) = 2.98 cm^{-1}. Intensity data $\pm h,k,l$; 2445 nonequivalent reflections (θ_{max} = 45°); R = 0.046 (R_w = 0.061, GOF = 2.79) over 2152 reflections with $I > 3.0\sigma(I)$.

(15) (a) [Li(HMDS)·1THF]$_2$: Englehardt, L. M.; Jolly, B. S.; Punk, P. C.; Raston, C. L.; Skelton, B. W.; White, A. H. *Aust. J. Chem.* **1986**, *39*, 133. (b) [Li(HMDS)·1Et$_2$O]$_2$: Lappert, M. F.; Slade, M. J.; Singh, A.; Atwood, J. L.; Rogers, R. D.; Shakir, R. *J. Am. Chem. Soc.* **1983**, *105*, 302–304. Engelhardt, L. M.; May, A. S.; Raston, C. L.; White, A. H. *J. Chem. Soc., Dalton Trans.* **1983**, 1671.

(16) (a) [K(HMDS)·2toluene]$_2$: Williard, P. G. *Acta Crystallogr.* **1988**, *C44*, 270–272. (b) [K(HMDS)]$_2$: Tesh, K. F.; Hanusa, T. P.; Huffman, J. C. *Inorg. Chem.* **1990**, *29*, 1584–1586. (c) [K(HMDS)·1THF]$_2$, [K(HMDS)·2THF]$_2$, [K(HMDS)·1($Me_2NCH_2CH_2NMe_2$)]$_2$: Williard, P. G.; Nichols, M. A., unpublished results.

(17) Single crystals of Li(HMDS)·K(HMDS)·3THF (**1**) were also isolated from an equimolar mixture of Li(HMDS) and potassium (+)-menthoxide in pentane/THF at −40 °C.

(18) Preliminary calorimetric studies of the enthalpies of deprotonation of combinations of lithium and potassium *tert*-butoxides mixed with Li(HMDS) and K(HMDS) in pure THF at 25 °C have been performed: Arnett, E. M.; Moe, K. D., personal communication.

Registry No. 1 (coordinate entry), 137203-49-7; **1** (salt entry), 137203-52-2; **2** (coordinate entry), 137203-50-0; **2** (salt entry), 137203-53-3; **3** (coordinate entry), 137203-51-1; **3** (salt entry), 137203-54-4.

Supplementary Material Available: Atomic numbering schemes and tables of crystallographic data, atomic positional and thermal parameters, bond lengths and angles, and selected torsion angles for the three mixed-alkali HMDS dimers **1-3** (44 pages). Ordering information is given on any current masthead page.

29-Methylidene-2,3-oxidosqualene: A Potent Mechanism-Based Inactivator of Oxidosqualene Cyclase

Xiao-yi Xiao and Glenn D. Prestwich*

Department of Chemistry, State University of New York Stony Brook, New York 11794-3400

Received July 26, 1991

The cyclization of (3*S*)-2,3-oxidosqualene to lanosterol by oxidosqualene cyclase (OSC) (EC 5.4.99.7) has fascinated organic chemists for over 30 years.[1] Substrate studies using crude liver microsomes suggested that partially cyclized cationic species were involved in the enzymatic mechanism.[2] Inhibitors of OSC have been examined with crude solubilized microsomes with OSC activity from plants, fungi, and vertebrates[3] and in cell culture systems.[4] The known OSC inhibitors include (i) substrate mimics (e.g., 2,3-iminosqualene[5]), (ii) product mimics (e.g., the decalols[6]), or (iii) transition-state analogues.[7] The last group includes mimics of the initial acyclic C-2 cation as well as mimics of partially cyclized bicyclic cations.[8] However, as yet, no irreversible inhibitors have been reported. We describe herein the synthesis and biological activity of 29-methylidene-2,3-oxidosqualene (29-MOS, **1a**), the first mechanism-based irreversible inactivator of OSC.

Scheme I summarizes the synthesis of the 26- and 29-methylidene-2,3-oxidosqualenes and the corresponding bis(epoxide).[9] Aldehydes **2a** and **2b**[10] were converted[11] to the unsaturated esters **3a,b** (*Z*:*E* = 44:1) and reduced, and the allylic alcohols were separated to give 26-hydroxysqualene (**4**). The two terminal monobromohydrins **5a** (11%) and **5b** (30%) and the bis(bromohydrin) **5c** (13%) were processed independently by base-induced oxirane formation, allylic oxidation,[12] and olefination to provide the isomeric 29-MOS (**1a**) and 26-MOS (**1b**) and bis(epoxide) **1c**.

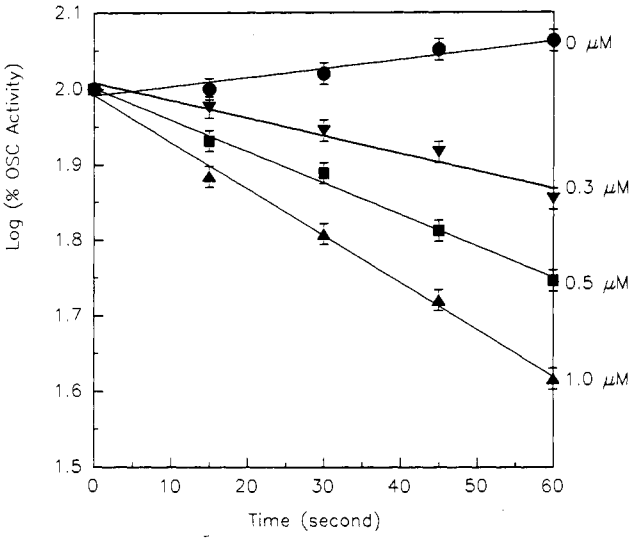

Figure 1. Time dependency of inactivation of pig liver microsomal OSC by 29-MOS (**1a**).

Enzyme assays to measure inhibition of OSC used [^{14}C]-(3*S*)-2,3-oxidosqualene[13] as substrate and either solubilized microsomal protein from pig liver[14] or a sonicated bakers' yeast suspension.[15] Conversion was determined by radio-TLC, and reversibility was determined using DEAE chromatography to separate the enzyme from the inhibitor.[16] The IC_{50} values for inhibition of liver OSC at 20 μM substrate were determined to be 0.5, 78, and 1.6 μM for **1a**, **1b**, and **1c**, respectively.[17] Note that methylidene substitution at the 26-position is 100-fold less potent than at the 29-position, but the 22,23-epoxide only reduces the potency of 29-MOS 3-fold. Most importantly, only the 29-substituted 2,3-epoxide **1a** and the bis(epoxide) **1c** showed irreversible inhibition of OSC.

The inhibition of microsomal OSC by 29-MOS (**1a**) showed an apparent K_I value of 4.4 μM. The time dependence of inhibition at [29-MOS] = 1, 0.5, and 0.3 μM allowed determination of the k_{inact} value of 221 min^{-1} for liver OSC (Figure 1),[18] of the same magnitude as that expected for k_{cat} for oxidosqualene. A partition ratio of 3.8 was calculated for 29-MOS by measuring the decrease in OSC activity at increasing 29-MOS concentrations.

Cyclization reactions of [^{3}H]-29-MOS (**1a**, T = ^{3}H), [^{3}H]-**1b**, and [^{3}H]-**1c** were followed by radio-TLC.[19] Incubation of 0.1 μM [^{3}H]-29-MOS (specific activity = 2.3 Ci/mmol[19]) with pig liver microsomes or with sonicated bakers' yeast suspension gave a new polycyclic product in yields of 30% and 15%, respectively. At [29-MOS] > K_I, complete inactivation precluded isolation of product. On the basis of the regiospecificity of the methylidene substitution for inhibition, we propose that this product is the 21-methylidenelanosterol. Similarly, cyclization of **1b** also gave

(1) (a) Stork, G.; Burgstahler, A. W. *J. Am. Chem. Soc.* **1955**, *77*, 5068-5077. (b) Stadler, P. G.; Eschenmoser, A.; Shenz, H.; Stork, G. *Helv. Chim. Acta* **1957**, *40*, 2191-2198. (c) Johnson, W. S. *Acc. Chem. Res.* **1968**, *1*, 1-8. (d) Johnson, W. S. *Bioorg. Chem.* **1976**, *5*, 51-98. (e) van Tamelen, E. E. *Acc. Chem. Res.* **1975**, *8*, 152-160.

(2) van Tamelen, E. E. *J. Am. Chem. Soc.* **1982**, *104*, 6480-6481,

(3) Cattel, L.; Ceruti, M.; Balliano, G.; Viola, F.; Grosa, G.; Schuber, F. *Steroids* **1989**, *53*, 363-391.

(4) Popjak, G.; Meenan, A.; Nes, W. D. *Proc. R. Soc. London, B* **1987**, *232*, 273-287.

(5) Corey, E. J.; Ortiz de Montellano, P. R.; Lin, K.; Dean, P. D. G. *J. Am. Chem. Soc.* **1967**, *89*, 2797-2799.

(6) (a) Nelson, J. A.; Czarny, M. R.; Spencer, T. A.; Limanek, J. S.; McCrae, K. R.; Chang, T.-Y. *J. Am. Chem. Soc.* **1978**, *100*, 4900-4902. (b) Chang, T.-Y.; Schiavoni, E. S.; McCrae, K. R.; Nelson, J. A.; Spencer, T. A. *J. Biol. Chem.* **1979**, *254*, 11258-11264. (c) Raveendranath, P. C.; Newcomb, L. F.; Ray, N. C.; Clark, D. S.; Spencer, T. A. *Synth. Commun.* **1990**, *20*, 2723-2733.

(7) Ceruti, M.; Delprino, L.; Cattel, L.; Bouvier-Navé, P.; Duriatti, A.; Schuber, F.; Benveniste, P. *J. Chem. Soc., Chem. Commun.* **1985**, 1054-1055.

(8) Duriatti, A.; Bouvier-Navé, P.; Benveniste, P.; Schuber, F.; Delprino, L.; Balliano, G.; Cattel, L. *Biochem. Pharmacol.* **1985**, *34*, 2765-2777.

(9) All compounds in Scheme I are racemic mixtures. New compounds have IR, NMR, and mass spectra fully consistent with the indicated structures. Full experimental details are provided in the supplementary material.

(10) Ceruti, M.; Viola, F.; Dosio, F.; Cattel, L.; Bouvier-Navé, P.; Ugliengo, P. *J. Chem. Soc., Perkin Trans. 1* **1988**, 461-469.

(11) Still, W. C.; Gennari, C. *Tetrahedron Lett.* **1983**, *24*, 4405-4407.

(12) (a) Xiao, X-y.; Prestwich, G. D. *Synth. Commun.* **1990**, *20*, 3125-3130; (b) Bai, M.; Xiao, X-y.; Prestwich, G. D. *Bioorg. Med. Chem. Lett.* **1991**, *1*, 227-232.

(13) Xiao, X-y.; Prestwich, G. D. *J. Labelled Compd. Radiopharm.* **1991**, *29*, 883-890.

(14) Sen, S. E.; Prestwich, G. D. *J. Med. Chem.* **1989**, *32*, 2152-2158.

(15) Bujons, J.; Guajardo, R.; Kyler, K. S. *J. Am. Chem. Soc.* **1988**, *110*, 604-606.

(16) Dialysis is ineffective in removing lipophilic inhibitors from OSC. Reactivation of squalene epoxidase inhibited by trisnorsqualene cyclopropylamine and other inhibitors was accomplished similarly: (a) Sen, S. E.; Prestwich, G. D. *J. Am. Chem. Soc.* **1989**, *111*, 8761-8762. (b) Bai, M.; Prestwich, G. D., submitted manuscript.

(17) For yeast OSC, IC_{50} values of 1.5 μM (**1a**), 19 μM (**1b**), and 11 μM (**1c**) were observed.

(18) Analyses were performed using Lineweaver-Burk and Kitz-Wilson plots. The K_I values for liver OSC were 122 μM (**1b**) and 7.1 μM (**1c**); the k_{inact} value for **1c** was 113 min^{-1}. Assays with **1a** and **1c** with short (10, 30, 45, 60 s) incubation periods were required to obtain these data.

(19) High specific activity [^{3}H]-29-MOS had to be used to detect cyclization at this low concentration. Reduction of **7a** (T = H) with [^{3}H]sodium borohydride to **6a** (T = ^{3}H), oxidation, and methylenation gave 5.4 mCi of [^{3}H]-29-MOS (2.3 Ci/mmol).

0002-7863/91/1513-9673$02.50/0